Transportation Research Part C 120 (2020) 102828

Contents lists available at ScienceDirect

Transportation Research Part C

journal homepage: www.elsevier.com/locate/trc

Max-pressure signal control with cyclical phase structure

Michael W. Levin *, Jeffrey Hu, Michael Odell

Department of Civil, Environmental, and Geo-Engineering, University of Minnesota, United States of America

ARTICLE INFO

Keywords:
Max-pressure control
Traffic signal
Signal cycle
Decentralized

ABSTRACT

Max-pressure traffic signal control has many desirable properties. It is analytically proven to maximize network throughput if demand could be served by any signal control. Despite its network-level stability properties, the control itself is decentralized and therefore easily computed by individual intersection controllers. Discussions with city engineers have suggested that a major barrier to implementation in practice is the non-cyclical phase actuation of max-pressure control, which can actuate any phase, in arbitrary order, to serve the queue(s) with highest pressure. This arbitrary phase selection may be confusing to travelers expecting a signal cycle, and is therefore unacceptable to some city traffic engineers. This paper revises the original max-pressure control to include a signal cycle constraint. The max-pressure control must actuate an exogenous set of phases in order, with each phase actuated at least one time step per cycle. Each cycle has a maximum length, but the length can be reduced if desired. Within those constraints, we define a modified max-pressure control and prove its maximum stability property. The revised max-pressure control takes the form of a model predictive control with a one cycle lookahead, but we prove that the optimal solution can be easily found by enumerating over phases. The policy is still decentralized. Numerical results show that as expected, the cyclical max-pressure control performs slightly worse than the original max-pressure control due to the additional constraints, but with the advantage of greater palatability for implementation in practice.

1. Introduction

Intersections are a major bottleneck for urban networks. To optimize traffic signal timings, recent studies (Wongpiromsarn et al., 2012; Varaiya, 2013; Le et al., 2015) proposed max-pressure control techniques which use observed queue lengths to adaptively adjust signal timings. The key desirable properties of max-pressure control are *maximum stability*, i.e. max-pressure control is analytical proven to serve all demand if the demand could be served by *any* signal timing. Another nice property is *decentralized control*, in which the network-wide optimal solution can be found by a local computation at each intersection that depends only on the immediately upstream and downstream links.

Given these favorable characteristics, we seek to resolve a major practical issue that discourages implementation by city engineers. Specifically, drivers prefer traffic signals to follow a cyclical phase structure. Most work on max-pressure control (building off Wongpiromsarn et al., 2012; Varaiya, 2013) use a time step-based phase selection. (Le et al., 2015, has a signal cycle, but the cycle length is fixed and phase durations can be arbitrarily small.) Although a non-cyclical phase selection may improve throughput, the limitations include potentially unbounded waiting times and the appearance of phases being "skipped" for waiting drivers. Due to the need to also serve pedestrians, and the desire to avoid complaints about phase skipping from drivers, city engineers in Minnesota

* Corresponding author.
E-mail address: mlevin@umn.edu (M.W. Levin).

https://doi.org/10.1016/j.trc.2020.102828
Received 27 April 2020; Received in revised form 30 September 2020; Accepted 1 October 2020
Available online 12 October 2020

have criticized the lack of a signal cycle during discussions about implementing max-pressure control in practice. Instead of leaving this issue to be addressed by practitioners in an ad-hoc practical sense that obviates the analytical properties, this paper aims to develop the maximum stability properties of max-pressure control under the constraint that phases follow a signal cycle structure.

The contributions of this paper are as follows: We modify Varaiya (2013)'s max-pressure control model and policy to follow a signal cycle with a maximum cycle length. The cycle length is adaptive with a maximum value. Each phase must be actuated at least once in order during each cycle. The cycle length constraint restricts the size of the stable region, but we prove that the new max-pressure policy still has maximum stability (among signal timings that also follow the cycle length constraint). The resulting policy takes the form of a model predictive control, but we prove the equivalence of a simpler one-time step solution method. Numerical results compare delays and throughput for max-pressure control with and without the cyclical structure constraints.

The remainder of this paper is organized as follows. Section 2 reviews previous work on max-pressure policies for intersection control. Section 3 defines and proves the stability properties of a cycle-based max-pressure control. Numerical results on the downtown Austin city network are presented in Section 4, and we conclude in Section 5.

2. Literature review

The max pressure algorithm was initially developed for wireless network packet transmission by Tassiulas and Ephremides (1992). In recent years, there have been several publications adapting max pressure control to signalized intersections. Gregoire et al. (2014a) and Varaiya (2013) defined max-pressure control and proved its stability for store-and-forward queueing models, which are similar to the point queue model for traffic flow. Recognizing that point queues are not a realistic model of traffic flow, Xiao et al. (2014) proved the stability of a max-pressure control policy for a network of spatial queues. Gregoire et al. (2014b) also studied max-pressure control within spatial queues, but did not prove the stability of their policy. Li and Jabari (2019) used a continuous time model to obtain a provably-stable max-pressure control using kinematic wave theory for traffic flow, although the density function must be known exactly to solve the policy.

Several papers have used max-pressure techniques for novel technologies. Le et al. (2017) seeks to influence drivers' behavior in order to increase network efficiency. Rey and Levin (2019) studied max-pressure control for autonomous vehicle intersection management, with the goal of providing human-driven vehicles access to the intersection in a throughput-optimal fashion. Chen et al. (2020) reported a similar result for throughput-optimal pedestrian access. Levin et al. (2019) used max-pressure control to optimize dynamic lane reversal with autonomous vehicle intersection control. All aforementioned papers include proofs of stability.

The max-pressure policy is complex and not all previous studies have included an analytical proof of stability. Instead, simulations have been used to show the effectiveness of implementation. Sun and Yin (2018) compared max-pressure control to coordinated actuated traffic signals in VISSIM, with very favorable results. Mercader et al. (2020) and Dixit et al. (2020) studied pressure-based policies using travel times instead of queue lengths through experiments on real traffic, showing improvements in flow and delay, respectively. Since analytical stability establishes maximum throughput when demand is in the stable region, but does not otherwise compare delays or other performance metrics, such simulation and experimental results are valuable for evaluating the benefits.

The most similar previous studies to this one also considered a cycle-based signal selection with the aim of actuating each of a predefined set of phases in order each cycle. Many previous studies building off Varaiya (2013)'s model can actuate phases in random order, without any concept of a signal cycle. Le et al. (2015) specified the time step to be one signal cycle, instead of selecting one phase per time step like most previous studies. The advantages to this approach include potentially allocating any real number time to each phase, as opposed to being limited to integer numbers of time steps per phase. However, there does not appear to be a minimum time allocated to each phase in their model, which may reduce the usability of green phases due to the startup delay. Like this paper, Pumir et al. (2015) and Anderson et al. (2018) actuated one phase per time step, and required that each phase be actuated once per signal cycle for some minimum time. Unlike this paper, their signal cycles had fixed duration, which has two disadvantages. Due to lost time, longer cycles are needed to increase capacity, but shorter cycles can achieve smaller waiting times. A fixed cycle length requires a fixed, rather than demand-responsive, approach to balancing capacity against waiting times. Second, their phase durations for the entire cycle are determined at the start of the cycle, which means that the arrival of vehicles does not immediately affect the signal phase. These two issues are addressed by this paper, which develops a model predictive control cycle-based max-pressure policy with adaptive cycle length.

3. Methodology

We define a maximum-stability traffic signal phase policy that obeys the constraints of cyclical phase selection. *Stability* refers to the property of serving all demand. If demand is unserved, then the number of vehicles in the network will increase in expectation over time. In contrast, if the network is stable, then the throughput is equal to the input rate of demand. These qualitative definitions will be made more clear by the analytical development in this section.

Like most work on max-pressure intersection control, the methodology proceeds along several steps. First, we construct a store-and-forward queueing model to represent the traffic network, with modifications for cyclical phase selection. Using this model, we define analytically the set of demand rates that could be served by any traffic signal timing. We then provide a signal phase policy that serves any stabilizable demand, and prove its stability properties.

3.1. Network model

Consider a network $\mathcal{G} = (\mathcal{N}, \mathcal{A})$ with nodes $\mathcal{N}$ and directed links $\mathcal{A}$. The set of nodes is divided into junctions $\mathcal{N}_{\mathrm{i}}$ and centroids $\mathcal{N}_{\mathrm{z}}$. The set of links is divided into internal links $\mathcal{A}_{\mathrm{i}}$ and entry links $\mathcal{A}_{\mathrm{e}}$. Entry links connect a centroid to a junction. Internal links connect two junctions. All vehicles enter the network on an entry link and travel through the network until reaching their destination centroid. Route choice is modeled through exogenous turning proportions.

Consider discretized time. Assume without loss of generality that each link takes 1 time step to traverse at free flow. (Longer links can be divided into shorter segments.) Like previous work on max-pressure signal control (Varaiya, 2013; Le et al., 2015), we track the evolution of queue lengths per link using a store-and-forward queueing model. Let $x_{ij}(t)$ be the number of vehicles on link i waiting to move to link j. Link queues are separated by turning movements because different turning movements may not be actuated simultaneously during a traffic signal. Link queues evolve via conservation of flow. For internal links, flow conservation results in

$$x_{jk}(t+1) = x_{jk}(t) - y_{jk}(t) + \sum_{i \in \mathcal{A}} y_{ij}(t) r_{jk}(t) \tag{1a}$$

where $y_{jk}(t)$ is the flow of vehicles from j to k at time t, which is controlled by traffic signal actuation. Turning proportions $r_{jk}(t)$ determine the proportion of vehicles entering j that will next move to k. We assume that $r_{jk}(t)$ are independent identically distributed random variables with mean $\bar{r}_{jk}$. Flow conservation also applies to entry links, but entering flow is determined by the demand $d_i(t)$.

$$x_{ij}(t+1) = x_{ij}(t) - y_{ij}(t) + d_i(t) r_{ij}(t) \tag{1b}$$

We assume that for each entry link $i \in \mathcal{A}_{\mathrm{e}}$, $d_i(t)$ for all t are independent identically distributed random variables with mean $\bar{d}_i$. We further assume that $d_i(t)$ has a maximum value $\tilde{d}_i$, which is reasonable because centroids are likely to have a physical capacity limitation. The queue length state $\mathbf{x}(t)$ forms a Markov chain with stochasticity due to the random demand $\mathbf{d}(t)$ and turning proportions $\mathbf{r}(t)$.

Intersection flows $y_{ij}(t)$ are controlled by the traffic signal activation. At each time step, a traffic signal phase is selected. Let $s_{ij}(t) \in \{0, 1\}$ indicate whether turning from (i, j) is permitted at time step t. Then $y_{ij}(t)$ is defined by

$$y_{ij}(t) = \min\left\{x_{ij}(t), s_{ij}(t) Q_{ij} [1 - L_{ij}(t)]\right\} \tag{2}$$

where Q_{ij} is the capacity of turning movement (i, j). We assume that Q_{ij} is bounded. The term $1 - L_{ij}(t)$ reduces capacity by the lost time $L_{ij}(t)$ when the time is in units of 1 time step. We model lost time $L_{ij}(t)$ as a function of the phase selection. For instance, if the same phase is selected for two consecutive time steps, then lost time is 0 during the second of those time steps. When a phase changes, then positive lost time may be added to model the all-red and startup delay intervals. We assume that $0 \leq L_{ij}(t) \leq 1$ time step.

3.2. Traffic signal cycle

The network model defined in Section 3.1 is very similar to Varaiya (2013)'s model. The key difference that we explore in this paper is constraining the traffic signal phase selection to follow a cycle. Although constraints on phase selection reduce the throughput of the max-pressure policy, practical requirements encourage the use of a signal cycle. For instance, many drivers expect signals to follow a cycle, and might become frustrated or confused if phases appear in seemingly random order as they might using Varaiya (2013)'s max-pressure policy. Furthermore, drivers expect to have a maximum waiting time to receive a green light. For these reasons, city traffic engineers are unwilling to implement Varaiya (2013)'s signal phase selection directly, despite the throughput benefits.

Although Le et al. (2015) assigned green time using a max-pressure policy, they required a fixed cycle length. Furthermore, green time could become arbitrarily close to 0 as the pressure increased. In this paper, we assume that the minimum green time for each phase is one time step. Like adaptive traffic signals, the cycle length can also change in response to the actual realization of demand.

Each turning movement (i, j) is uniquely associated with one node n, where i is an incoming link and j is an outgoing link. Let $\mathcal{M}_n$ be the set of turning movements associated with n. Let $\mathcal{P}_n$ be the ordered set of phases comprising the signal cycle for n. Let $p_n(t) \in \left[1, |\mathcal{P}_n|\right]$ be the phase number actuated at time step t for node n. Phases directly determine the turning movement activation $s_{ij}(t)$. Let $\xi_{ij}^{p} \in \{0, 1\}$ indicate whether phase p activates movement (i, j). Then

$$s_{ij}(t) = \xi_{ij}^{p_n(t)} \tag{3}$$

We assume that phases must be actuated in the specified order. To satisfy that, the phase at time step t is either the phase at $t - 1$ or the next phase in the cycle:

$$p_n(t) \in \left\{p_n(t-1), p_n(t-1) + 1\right\} \tag{4}$$

With a concrete definition of phases, we can explicitly define $L(\mathbf{s}(t))$:

$$L_{ij}(t) = \begin{cases} \tilde{L}_n & p_n(t) \neq p_n(t-1) \\ 0 & p_n(t) = p_n(t-1) \end{cases} \tag{5}$$

Lost time is 0 when the phase remains the same from time $t-1$ to t, and equal to $\tilde{L}_n$, an exogenous constant per intersection n specifying the lost time (which may depend on intersection geometry or other factors).

Furthermore, each phase must be actuated for at least one time step each cycle. Let C_n be the maximum cycle length for intersection n. C_n is restricted to an integer number of time steps. Let $c_n(t)$ be the duration of time since the signal cycle started for node n at time step t. For example, if phase $p_n(t-1) = |\mathcal{P}_n|$ (the last phase in the cycle for n) was actuated at time step $t-1$, and $p_n(t) = 1$ (the first phase), then $c_n(t) = 0$ indicates that at time t the signal cycle was started for node n. More generally,

$$c_n(t+1) = \begin{cases} 1 & \text{if } p_n(t) = |\mathcal{P}_n| \text{ and } p_n(t+1) = 1 \\ c_n(t)+1 & \text{else} \end{cases} \tag{6}$$

To maintain a maximum cycle length, require that $c_n(t) \le C_n$ for all t. Since each phase is actuated for at least one time step, the maximum cycle length imposes a constraint on phase actuation:

$$p_n(t) \ge |\mathcal{P}_n| - (C_n - c_n(t)) \tag{7}$$

For example, suppose there is 1 time step remaining in the cycle, so $C_n - c_n(t) = 1$ with 3 phases total ($|\mathcal{P}_n| = 3$). Then constraint (7) requires that $p_n(t) \ge 3 - 1 = 2$. If $p_n(t) = 2$, then $p_n(t+1) = 3$ is possible, which would complete the cycle.

3.3. Stable region

We first define stability mathematically. The network is stable if the number of vehicles in the network remains bounded in expectation. Equivalently, there exists a $\kappa < \infty$ such that

$$\lim_{T\to\infty} \sup \left\{ \frac{1}{T} \sum_{t=1}^{T} \sum_{((i,j)\in\mathcal{A}^2)} \mathbb{E}\left[x_{ij}(t)\right] \right\} \le \kappa \tag{8}$$

It is easy to choose a demand rate vector $\bar{\mathbf{d}}$ such that no traffic signal timing policy can stabilize it (for instance, demand that exceeds turning movement capacity). The objective of max-pressure control is to stabilize any demand rate that could be stabilized by some signal control. To prove the maximum-stability property, we must first define analytically the set of demands that could be stabilized. Although the stability region is similar to that of Varaiya (2013), the constraint that phases follow an exogenous cycle affects the demand that can be served. Since demand is stochastic, the stable region is defined in terms of the average demand rates $\bar{\mathbf{d}}$.

Demand for entry links can be propagated to demand for internal links. Let f_i be the average traffic volume for link i. For entry links,

$$f_i = \bar{d}_i \tag{9a}$$

For internal links, f_i can be determined by conservation of flow:

$$f_j = \sum_{i\in\mathcal{A}} f_i \bar{r}_{ij} \tag{9b}$$

Actual flow rates of $\mathbf{f}$ can only be achieved if the network is stable, otherwise the capacity will be insufficient to admit flow of f_i on one or more links. The derivation of $\mathbf{f}$ from $\bar{\mathbf{d}}$ is useful because it analytically describes the average flow that must be served on each internal link in the network as well as the entry links. Notice that the equivalence of $\bar{\mathbf{d}}$ with $\mathbf{f}$ does not guarantee that flow of $\mathbf{f}$ will be realized. $\mathbf{f}$ does not represent average flow on links for unstable networks. $\mathbf{f}$ is merely the conversion of average entering demand $\bar{\mathbf{d}}$ and average turning proportions $\bar{\mathbf{r}}$ into link demand.

By Proposition 1 of Varaiya (2013), for every demand rate $\bar{\mathbf{d}}$ and turning proportions $\bar{\mathbf{r}}$, there exists an unique average flow vector $\mathbf{f}$. The network can be stabilized if the average traffic volume can be served by some signal control. Equivalently, there must exist an average signal activation $\bar{s}_{ij}$ and average lost time $\bar{L}_{ij}$ such that

$$f_i \bar{r}_{ij} \le \bar{s}_{ij} Q_{ij} \left(1 - \bar{L}_{ij}\right) \tag{10}$$

where

$$\bar{s}_{ij} = \lim_{T\to\infty} \frac{1}{T} \sum_{t=1}^{T} s_{ij}(t) \tag{11}$$

is the average signal activation time from the signal phase sequence $s_{ij}(t)$ and

$$\bar{L}_{ij} = \lim_{T\to\infty} \frac{1}{T} \sum_{t=1}^{T} L_{ij}(t) \tag{12}$$

is the average lost time. Since $s_{ij}(t)$ satisfies the signal cycle structure, certain bounds can be derived for $\bar{s}_{ij}$ and $\bar{L}_{ij}$. It is easier to define the proportion of time that each phase is activated, which we denote by λ_n^p for phase p of node n. λ_n^p satisfies

$$\sum_{p=1}^{|\mathcal{P}_n|} \lambda_n^p = 1 \tag{13}$$

Since each phase is activated at least once per cycle, $\lambda_n^p \geq \frac{1}{C_n}$ also. Then the upper bound can be derived from the number of phases, since phase p can be activated at most $C_n - |\mathcal{P}_n| - 1$ times:

$$\lambda_n^p \in \left[\frac{1}{C_n}, \frac{C_n - |\mathcal{P}_n| - 1}{C_n}\right] \tag{14}$$

Proposition 1. *For any λ_n satisfying constraint (14), there exists a phase sequence $p_n(t)$ with*

$$\lim_{T\to\infty} \frac{1}{T} \sum_{t=1}^{T} \mathbb{1}(p_n(t) = p) = \lambda_n^p \tag{15}$$

for all $p \in [1, |\mathcal{P}_n|]$ where $\mathbb{1}(\cdot)$ is the indicator function.

Proof. For any $\epsilon > 0$, for all $p \in [1, |\mathcal{P}_n|]$ there exists a rational number $\frac{k_p}{M} \in [\lambda_n^p - \epsilon, \lambda_n^p + \epsilon]$ with $\sum_{p=1}^{|\mathcal{P}_n|} k_p = 1$ since $\sum_{p=1}^{|\mathcal{P}_n|} \lambda_n^p = 1$. Then if each phase p is chosen k_p out of M times,

$$\left|\frac{1}{T} \sum_{t=1}^{T} \mathbb{1}(p_n(t) = p) - \lambda_n^p\right| = \left|\frac{k_p}{M} - \lambda_n^p\right| \leq \epsilon \tag{16}$$

because the rational numbers are dense in the real numbers, which achieves convergence to λ_n. □

Proposition 1 proves that λ_n^p in the set defined by Eq. (14) is attainable given a sufficiently long sequence of phase selections. Given λ_n^p, we can define $\bar{s}_{ij}$:

$$\bar{s}_{ij} = \sum_{p=1}^{|\mathcal{P}_n|} \lambda_n^p \xi_{ij}^p \tag{17}$$

Let S be the set of feasible average signal activation matrices $\bar{\mathbf{s}}$.

$$S = \left\{\bar{\mathbf{s}} : \bar{s}_{ij} = \sum_{p=1}^{|\mathcal{P}_n|} \lambda_n^p \xi_{ij}^p, \lambda_n^p \in \left[\frac{1}{C_n}, \frac{C_n - |\mathcal{P}_n| - 1}{C}\right], \sum_{p=1}^{|\mathcal{P}_n|} \lambda_n^p = 1\right\} \tag{18}$$

be the set of feasible average signal activations. $\bar{L}_{ij}$ is more difficult to define. However, given a number of phases $\mathcal{P}_n$, $\bar{L}_{ij}$ can be lower-bounded:

$$\bar{L}_{ij} \geq \frac{\tilde{L}_n \left|\left\{p_n : \xi_{ij}^{p_n} = 1 \text{ and } \xi_{ij}^{p_{n-1}} \neq 1\right\}\right|}{C_n} \tag{19}$$

For the purposes of defining the stable region, we assume that condition (19) holds with equality, meaning that the average control $\bar{\mathbf{s}}$ uses the minimum lost time. This is not limiting because decreasing the lost time increases the capacity as per equation. Therefore, a control $\bar{\mathbf{s}}$ with minimum lost time can stabilize any demand in the stable region. Let $\hat{Q}_{ij}$ be the maximum capacity from (i, j) determined by Eq. (19), i.e.

$$\hat{Q}_{ij} = Q_{ij}\left(1 - \frac{\tilde{L}_n \left|\left\{p_n : \xi_{ij}^{p_n} = 1 \text{ and } \xi_{ij}^{p_{n-1}} \neq 1\right\}\right|}{C_n}\right) \tag{20}$$

Every signal cycle of intersection n, when the phase switches from a phase p_{n-1} that does not activate (i, j) to a phase p_n that activates (i, j), lost time must be incurred. Assuming a maximum cycle length of C_n, the number of phase switches determines the lower bound on $\bar{L}_{ij}$. Since the order of phases is fixed, the quantity of lost time per cycle is also fixed. However, a larger average lost time could be achieved if the cycle duration is less than the maximum of C_n. Corollary 1 states that any λ_n can be achieved with a cycle length of C_n. Equivalently, the minimum $\bar{L}_{ij}$ can be achieved for any λ_n.

Corollary 1. *For any λ_n satisfying constraint (14), there exists a phase sequence $p_n(t)$ with*

$$\lim_{\Gamma\to\infty} \frac{1}{\Gamma} \sum_{\gamma=1}^{\Gamma} \frac{1}{C_n} \sum_{t=1}^{C_n} \mathbb{1}(p_n(t + \gamma C_n) = p) = \lambda_n^p \tag{21}$$

for all $p \in [1, |\mathcal{P}_n|]$ where $\mathbb{1}(\cdot)$ is the indicator function.

Proof. By Proposition 1, there exists a T such that

$$\lim_{T\to\infty} \frac{1}{T} \sum_{t=1}^{T} \mathbb{1}(p_n(t) = p) = \lambda_n^p \tag{22}$$

Repeating the sequence a discrete C_n times,

$$\lim_{T\to\infty} \frac{1}{TC_n} \sum_{t=1}^{TC_n} \mathbb{1}(p_n(t) = p) = \lambda_n^p \quad \square \tag{23}$$

Let D be the set of demand rates such that constraint (10) holds. D is the stability region, i.e. the set of demands such that some signal phase sequence provides enough average capacity to serve the average demand. When $\bar{\mathbf{d}}$ is on the boundary of D, the Markov chain representing the queueing model can be null recurrent but not positive recurrent. Therefore, consider the set D^0 which is the interior of D, i.e. where constraint (10) holds with strict inequality. Then there exists an $\epsilon > 0$ such that

$$f_i \bar{r}_{ij} - \bar{s}_{ij} Q_{ij} \left(1 - \bar{L}_{ij}\right) \le -\epsilon \tag{24}$$

We will define a max-pressure policy that stabilizes the network if $\bar{\mathbf{d}} \in D^0$, and use ϵ in the proof of stability.

Proposition 2. *If $\bar{\mathbf{d}} \notin D$, then there does not exist a signal control policy that can stabilize the network.*

The proof is analogous to Theorem 2 of Varaiya (2013). If $\bar{\mathbf{d}}$ and $\bar{\mathbf{r}}$ are known with $\bar{\mathbf{d}} \in D^0$, then it is easy to design a fixed signal timing that stabilizes the network. $\bar{\mathbf{r}}$ is often estimated for current signal timing practice (i.e. the proportion of vehicles making left and right turns). However, $\bar{\mathbf{d}}$ is more difficult to obtain. The adaptive max-pressure control in Section 3.4 can stabilize the network without knowing $\bar{\mathbf{d}}$.

3.4. Max-pressure policy

Because the max-pressure policy is constrained to follow a signal cycle, intuitively it must maintain some awareness of the current state of the cycle. This awareness is provided by defining an integer program that looks ahead for a planning horizon of $\mathcal{T}$. In this section, $\mathcal{T}$ is used to represent a planning horizon, whereas T is used at the end of the time horizon (so $\mathcal{T} \le T$). At time step t the integer program is solved on the horizon $t + \tau \in [t, t + \mathcal{T} - 1]$ and the first step of the solution is implemented. At time step $t + 1$ the integer program is again solved, and the (possibly) updated solution is used for time step $t + 1$.

First, define the weight for turning movement (i, j), $w_{ij}(t)$, as

$$w_{ij}(t) = x_{ij}(t) - \sum_{i\in\mathcal{A}} x_{jk}(t)\bar{r}_{jk} \tag{25}$$

This pressure has an intuitive interpretation of seeking to move vehicles from long queues to short queues. However, the precise form is analytically necessary for the stability proof.

Let $z_n^p(t) \in \{0, 1\}$ indicate whether phase p is activated for node n at time t. Notice that $z_n^p(t-1)$ is exogenous and determined by $p_n(t-1)$, specifically

$$z_n^p(t-1) = \begin{cases} 1 & p = p_n(t-1) \\ 0 & \text{else} \end{cases} \tag{26}$$

To ensure that only one phase is selected,

$$\sum_{p=1}^{|\mathcal{P}_n|} z_n^p(t+\tau) = 1 \qquad \forall n \in \mathcal{N}_{\mathrm{i}}, \forall \tau \in \left[0, \mathcal{T} - 1\right] \tag{27}$$

Since phases proceed in order, $z_p(t)$ is constrained by $z_p(t-1)$. Eq. (4) can be written as the following constraint:

$$z_n^p(t+\tau) \le z_n^p(t+\tau-1) + z_n^{p-1}(t+\tau-1) \qquad \forall n \in \mathcal{N}_{\mathrm{i}}, \forall \tau \in \left[0, \mathcal{T} - 1\right] \tag{28}$$

which requires that $z_n^p(t) = 1$ only if phase p or $p-1$ was active at time $t-1$. Since phases follow a cycle, when $p = 1$ phase $p-1$ refers to phase $|\mathcal{P}_n|$. The phase selection binary variables are also used to determine the lost time:

$$L_{ij}(t) = \bar{L}_{ij} \sum_{p=1}^{\mathcal{P}_n} \left(z_n^p(t) - z_n^p(t+1)\right) \qquad \forall n \in \mathcal{N}_{\mathrm{i}}, \forall \tau \in \left[0, \mathcal{T} - 1\right] \tag{29}$$

The term $z_n^p(t) - z_n^p(t+1)$ is equal to 1 only when the phase changes from p to $p+1$, and is equal to 0 otherwise.

Notice also that $c_n(t-1)$ is exogenous, and determines the number of time steps remaining before the maximum cycle length is reached. Let $\varphi_n(t) \in \{0, 1\}$ indicate whether the cycle restarts at time t for node n.

$$\varphi_n(t+\tau) \le z_n^1(t+\tau) - z_n^{|\mathcal{P}_n|}(t+\tau-1) \qquad \forall n \in \mathcal{N}_{\mathrm{i}}, \forall \tau \in \left[0, \mathcal{T} - 1\right] \tag{30}$$

which admits $\varphi_n(t) = 1$ only when the phase at node n switches from $|\mathcal{P}_n|$ to phase 1 from time $t-1$ to t. Let $c_n(t)$ be the number of time steps since the cycle was started, as defined by Eq. (6):

$$c_n(t+\tau) = \begin{cases} c_n(t+\tau-1) + 1 & \varphi_n(t+\tau) = 0 \\ 1 & \varphi_n(t+\tau) = 1 \end{cases} \qquad \forall n \in \mathcal{N}_{\mathrm{i}}, \forall \tau \in \left[0, \mathcal{T} - 1\right] \tag{31}$$

Constraints (31) can be linearized as

$$c_n(t+\tau) \geq c_n(t+\tau-1)+1-M\varphi_n(t+\tau) \qquad \forall n \in \mathcal{N}_{\mathrm{i}}, \forall \tau \in \left[0, \mathcal{T}-1\right] \tag{32a}$$

$$c_n(t+\tau) \leq c_n(t+\tau-1)+1+M\varphi_n(t+\tau) \qquad \forall n \in \mathcal{N}_{\mathrm{i}}, \forall \tau \in \left[0, \mathcal{T}-1\right] \tag{32b}$$

$$c_n(t+\tau) \geq 1-M(1-\varphi_n(t+\tau)) \qquad \forall n \in \mathcal{N}_{\mathrm{i}}, \forall \tau \in \left[0, \mathcal{T}-1\right] \tag{32c}$$

$$c_n(t+\tau) \leq 1+M(1-\varphi_n(t+\tau)) \qquad \forall n \in \mathcal{N}_{\mathrm{i}}, \forall \tau \in \left[0, \mathcal{T}-1\right] \tag{32d}$$

where M is a large positive constant. The maximum cycle length is enforced by the constraint

$$c_n(t+\tau) \leq C_n \qquad \forall n \in \mathcal{N}_{\mathrm{i}}, \forall \tau \in \left[0, \mathcal{T}-1\right] \tag{33}$$

Constraint (7) is included through the combination of constraints (31) and (33). Constraint (31) increments the cycle length timer $c_n(t+\tau)$ per time step, except when the cycle restarts by actuating the first phase. Constraint (33) restricts the maximum value of the cycle timer, which forces the cycle to restart for feasibility.

The final constraint relates $s_{ij}(t+\tau)$ with the phase selection:

$$s_{ij}(t+\tau) = \sum_{p=1}^{|\mathcal{P}_n|} z_n^p(t)\xi_{ij}^p \qquad \forall n \in \mathcal{N}_{\mathrm{i}}, \forall \tau \in \left[0, \mathcal{T}-1\right] \tag{34}$$

The max-pressure policy is found by solving the following integer linear program:

$$\max \qquad \frac{1}{\mathcal{T}} \sum_{\tau=0}^{\mathcal{T}-1} \sum_{(i,j)\in\mathcal{A}^2} s_{ij}(t+\tau) Q_{ij} \left(1-L_{ij}(t+\tau)\right) w_{ij}(t) \tag{35}$$

$$\text{s.t.} \qquad (27)\text{–}(30),\ (32a)\text{–}(34)$$

The optimal solution to problem (35) at time t, $\mathbf{s}^\star(t)$, is actuated at time step t. The remainder of the horizon of the optimal solution, $\mathbf{s}^\star(t+\tau)$ for $t \in \left[1, \mathcal{T}\right]$, is included only for planning purposes and discarded after actuating the solution at time t. Problem (35) essentially defines a model predictive control approach. The signal phase selection is optimized for $\mathcal{T}$ time steps ahead, and the first time step of the optimal solution is actuated.

Le et al. (2015) also studied a cyclical max-pressure policy. Unlike the policy (35), Le et al. (2015) assigns a time of $\frac{C_n \Delta t \exp\{\eta w_\sigma(t)\}}{\sum_{\pi\in\mathcal{P}_n} \exp\{\eta w_\pi(t)\}}$ where $w_\pi(t)$ is the weight for phase π at time t and η is an adjustment parameter. If the pressure for one phase is arbitrarily large (or small), then the proportion of the cycle length allocated to that phase can become arbitrarily close to C_n (or 0, respectively). In contrast, policy (35) will assign at least one time step to each phase per cycle, for a minimum of Δt and a maximum of $\Delta t(1-|\mathcal{P}_n|)$ time per cycle. However, this is but a side-effect of the main difference between these two policies. Le et al. (2015) has a fixed cycle length, whereas the cycle length of policy (35) can vary between $|\mathcal{P}_n|\Delta t$ and $C_n \Delta t$ via constraint (33).

Proposition 3. *The max-pressure control (35) has a decentralized solution.*

Proof. The optimal solution to problem (35) for any node n is independent of the decision variables at other nodes: the selection of $s_{ij}(t+\tau)$ and $L_{ij}(t+\tau)$ are independent of other nodes, and $w_{ij}(t)$ is exogenous. □

Problem (35) specifies decision variables for the entire network. However, the constraints can be separated by node, i.e. none of the constraints for decision variables for node n affect the decision variables for any other node n'. Consequently, problem (35) can be *decentralized*, i.e. it can be solved separately at each node for the phases specific to that node. Like other work on max-pressure control (Varaiya, 2013; Le et al., 2015), the decentralized property simplifies the solution method.

Having specified the max-pressure policy, the next step is to prove maximum stability, i.e. that if the network with demand rates of $\bar{\mathbf{d}}$ can be stabilized by some signal policy, then the max-pressure policy will stabilize the network. The goal of Proposition 4 and Lemma 1 is to establish that a planning horizon of $\mathcal{T} = C_n$ is sufficient. Proposition 4 also simplifies the solution to problem (35). Lemma 1 is directly used in the proof of stability. Proposition 4 is stated per node n because problem (35) can be decentralized by Proposition 3. The condition that lost time is minimized does not limit the proof of stability because minimizing lost time results in the largest stable region.

Proposition 4. *For each node n, define phase $p^\star$ as*

$$p^\star \in \underset{p\in[1,|\mathcal{P}_n|]}{\arg\max} \sum_{(i,j)\in\mathcal{M}_n} \xi_{ij}^p Q_{ij} w_{ij}(t) \tag{36}$$

When the lost time is equal to its minimum value, an optimal solution to

$$\max \frac{1}{C_n} \sum_{\tau=0}^{C_n-1} \sum_{(i,j)\in\mathcal{M}_n} s_{ij}(t+\tau) Q_{ij} \left(1-L_{ij}(t+\tau)\right) w_{ij}(t) \tag{37}$$

is to actuate $p^\star$ for $C_n - \left(|\mathcal{P}_n|-1\right)$ time steps out of C_n.

Proof. During any C_n consecutive time steps, each phase is actuated at least once because C_n is the maximum cycle duration. Ignore the positive constant $\frac{1}{C_n}$, then $\sum_{\tau=0}^{C_n-1}\sum_{(i,j)\in\mathcal{M}_n} s_{ij}(t+\tau)Q_{ij}\left(1-L_{ij}(t+\tau)\right)w_{ij}(t)$ can be rewritten as

$$\sum_{\tau=0}^{C_n-1}\sum_{(i,j)\in\mathcal{M}_n} s_{ij}(t+\tau)Q_{ij}\left(1-L_{ij}(t+\tau)\right)w_{ij}(t)$$
$$=\sum_{p=1}^{\mathcal{P}_n}\sum_{(i,j)\in\mathcal{M}_n}\xi_{ij}^{p}Q_{ij}(1-\tilde{L}_n)w_{ij}(t)+\sum_{\tau=0}^{C_n-|\mathcal{P}_n|}\sum_{(i,j)\in\mathcal{M}_n}\sum_{p\in\mathcal{P}_n} z_n^p(t+\tau)\xi_{ij}^{p}Q_{ij}w_{ij}(t) \tag{38}$$

where $L_{ij}(t+\tau)=0$ in the second part of the right hand side because the lost time is minimized. Since the term $\sum_{p=1}^{\mathcal{P}_n}\sum_{(i,j)\in\mathcal{M}_n}\xi_{ij}^{p}Q_{ij}(1-\tilde{L}_n)w_{ij}(t)$ is common to any feasible policy, the objective is to maximize $\sum_{\tau=0}^{C_n-|\mathcal{P}_n|}\sum_{(i,j)\in\mathcal{M}_n}\sum_{p\in\mathcal{P}_n} z_n^p(t+\tau)\xi_{ij}^{p}Q_{ij}w_{ij}(t)$.

$$\sum_{\tau=0}^{C_n-|\mathcal{P}_n|}\sum_{(i,j)\in\mathcal{M}_n}\sum_{p\in\mathcal{P}_n} z_n^p(t+\tau)\xi_{ij}^{p}Q_{ij}w_{ij}(t)\le\sum_{\tau=0}^{C_n-|\mathcal{P}_n|}\sum_{(i,j)\in\mathcal{M}_n}\xi_{ij}^{p^\star}Q_{ij}w_{ij}(t) \tag{39}$$
$$=\left(|\mathcal{P}_n|-C_n\right)\sum_{(i,j)\in\mathcal{M}_n}\xi_{ij}^{p^\star}Q_{ij}w_{ij}(t) \tag{40}$$

which is the simplified policy. □

Proposition 4 provides a simple solution to problem (35): find the phase

$$\mathbf{s}^\star=\arg\max\left\{\sum_{(i,j)\in\mathcal{A}^2} s_{ij}Q_{ij}w_{ij}(t)\right\} \tag{41}$$

and actuate it as soon as possible, following the signal cycle. Since the set of phases per intersection is exogenous and finite, this can be solved by enumeration.

Lemma 1 is used to compare the max-pressure policy to the average stabilizing control $\bar{\mathbf{s}}$. Lemma 1 may initially seem obvious, but is interesting for two reasons. First, $s_{ij}^\star(t)\in\{0,1\}$ whereas $\bar{s}_{ij}\in[0,1]$, so $\bar{s}_{ij}$ may not be in the feasible region of $s_{ij}(t)$. Second, Lemma 1 establishes that a planning horizon of $\mathcal{T}=C_n$ is sufficiently long to achieve stability.

Lemma 1. *Let $\mathbf{s}^\star(t+\tau)$, $\tau\in[0,C_n-1]$ be the optimal solution to (35). Assume the signal control is chosen with minimum lost time. Then for any node n,*

$$\frac{1}{C_n}\sum_{\tau=0}^{C_n-1}\sum_{(i,j)\in\mathcal{A}^2} s_{ij}^\star(t+\tau)Q_{ij}(1-L_{ij}(t))w_{ij}(t)\ge\sum_{(i,j)\in\mathcal{A}^2}\bar{s}_{ij}Q_{ij}(1-L_{ij}(t))w_{ij}(t) \tag{42}$$

Proof. By Proposition 4,

$$\frac{1}{C}\sum_{\tau=0}^{C-1}\sum_{(i,j)\in\mathcal{A}^2} s_{ij}^\star(t+\tau)Q_{ij}w_{ij}(t)=\frac{\sum_{p=1}^{|\mathcal{P}_n|}\sum_{(i,j)\in\mathcal{M}_n}\xi_{ij}^{p}Q_{ij}(1-L_{ij}(t))w_{ij}(t)+\left(C-|\mathcal{P}_n|\right)\sum_{(i,j)\in\mathcal{M}_n}\xi_{ij}^{p^\star}Q_{ij}w_{ij}(t)}{C} \tag{43}$$
$$\ge\sum_{p=1}^{|\mathcal{P}_n|}\sum_{(i,j)\in\mathcal{M}_n}\lambda_n^p\xi_{ij}^{p}\hat{Q}_{ij}w_{ij}(t) \tag{44}$$

for any $\sum_{p=1}^{|\mathcal{P}_n|}\lambda_n^p=1$ because the optimal solution is to provide as much cycle time as possible to phase $p^\star$. By Proposition 1, any $\bar{s}_{ij}$ corresponds to a λ_n satisfying $\sum_{p=1}^{|\mathcal{P}_n|}\lambda_n^p=1$, which establishes inequality (42). □

Note that the proposed method does not always choose the maximum cycle length because the model predictive control algorithm is updated at each time step. It is optimal in the model predictive control to actuate the phase with highest pressure for as long as possible. However, since the pressure is likely to decrease once a phase is actuated, at the next time step a different phase may have the highest pressure instead, which results in a phase switch. Actuating the highest pressure phase for a maximum cycle length occurs only when queues are so long that the phase pressure remains high after a full cycle length. When queues are shorter, cycle lengths will also decrease as phase switching occurs more frequently. Therefore, the cycle length adapts to the observed queues.

If $w_{ij}(t)$ were replaced with $w_{ij}(t+\tau)$ in problem (35), then The stability proof should follow easily. The disadvantage in using $w_{ij}(t+\tau)$ is that predicting $w_{ij}(t+\tau)$ is not so easy. By definition, $w_{ij}(t+\tau)=x_{ij}(t+\tau)-\sum_{i\in\mathcal{A}}x_{jk}(t+\tau)\bar{r}_{jk}$, so we must estimate $x_{ij}(t+\tau)$. Given the queue dynamics of Eq. (1a), the obvious estimation is

$$\mathbb{E}\left[x_{jk}(t+\tau)\right]=\mathbb{E}\left[x_{jk}(t+\tau-1)-y_{jk}(t+\tau-1)+\sum_{i\in\mathcal{A}}y_{ij}(t+\tau-1)r_{jk}(t+\tau-1)\right] \tag{45}$$

For node j, this requires calculating $\mathbb{E}\left[y_{ij}(t+\tau-1)\right]$, i.e. the expected incoming flow. Estimating the incoming flow can be split into two parts. First, if link (i,j) is an internal link, then $y_{ij}(t+\tau-1)$ is determined by the signal control $s_{ij}(t+\tau-1)$, which is a decision

variable in problem (35). That removes the decentralized property. Second, if link (i,j) is an entry link, then $\mathbb{E}\left[y_{ij}(t)\right] = \bar{d}_i \bar{r}_{ij}$, which requires knowledge of the demand. Another way of calculating $\mathbb{E}\left[y_{ij}(t+\tau-1)\right]$ is to use the stable region flows $f_i \bar{r}_{ij}$, but computing f_i requires knowing the average demand. Determining the average demand requires extensive work across the network, whereas installing a single max-pressure controller ideally requires only vehicle detectors on the incoming links. Furthermore, fluctuations in the daily average demand due to random events (such as weather patterns) would result in prediction errors unless the average demands were accurately adjusted. To summarize, we use $w_{ij}(t)$ instead of $w_{ij}(t+\tau)$ to reduce the data requirements and retain the decentralized property.

3.5. Maximum stability property

We now proceed to prove the maximum stability property of the proposed max-pressure control. We establish that if $\bar{\mathbf{d}} \in D^0$, then the max-pressure policy will stabilize the network. Due to Proposition 2, if $\bar{\mathbf{d}} \notin D$, then no signal timing policy can achieve stability. At the boundary of D, null recurrence to a stable state can be achieved, but not positive recurrence. Therefore, Propositions 2 and 5 together establish maximum stability. We first prove two supporting lemmas, then establish Proposition 5. Let $C = \max_n \in \mathcal{N}_i \{C_n\}$ be the maximum of the maximum cycle lengths of all intersections.

Lemma 2. *For any control* **s**, *if*

$$\exists \kappa_1 < \infty \ s.t. \ \mathbb{E}\left[\sum_{(i,j)\in\mathcal{A}^2} (x_{ij}(t+1))^2 - (x_{ij}(t))^2 \middle| \mathbf{x}(t)\right] \le \kappa_1 - \epsilon|\mathbf{x}(t)| \tag{46}$$

then

$$\exists \kappa_2 < \infty \ s.t. \ \frac{1}{C}\sum_{\tau=1}^{C} \mathbb{E}\left[\sum_{(i,j)\in\mathcal{A}^2} (x_{ij}(t+\tau+1))^2 - (x_{ij}(t))^2 \middle| \mathbf{x}(t+\tau)\right] \le \kappa_2 - \epsilon|\mathbf{x}(t)| \tag{47}$$

Proof. By Eq. (46),

$$\frac{1}{C}\sum_{\tau=1}^{C} \mathbb{E}\left[\sum_{(i,j)\in\mathcal{A}^2} (x_{ij}(t+\tau+1))^2 - (x_{ij}(t))^2 \middle| \mathbf{x}(t+\tau)\right] \le \frac{1}{C}\sum_{\tau=1}^{C} \kappa_1 - \epsilon|\mathbf{x}(t+\tau)| \tag{48}$$

$$\le \frac{1}{C}\sum_{\tau=1}^{C} \kappa_1 - \epsilon \sum_{(i,j)\in\mathcal{A}^2} \left(x_{ij}(t) - CQ_{ij}\right) \tag{49}$$

$$\le \kappa_2 - \epsilon \sum_{(i,j)\in\mathcal{A}^2} \left(x_{ij}(t)\right) \tag{50}$$

$$= \kappa_2 - |\mathbf{x}(t)| \tag{51}$$

because $x_{ij}(t+\tau) - x_{ij}(t) \ge -CQ_{ij}$. □

Lemma 3 establishes the main bounds on the Lyapunov function when the max-pressure control is used.

Lemma 3. *When the max-pressure policy is used with* $\bar{\mathbf{d}} \in D^0$,

$$\mathbb{E}\left[\frac{1}{C}\sum_{\tau=1}^{C}\sum_{(i,j)\in\mathcal{A}^2} (x_{ij}(t+\tau+1))^2 - (x_{ij}(t+\tau))^2 \middle| \mathbf{x}(t)\right] \le \kappa - \epsilon|\mathbf{x}(t)| \tag{52}$$

Proof. Let $\delta_{ij}(t) = x_{ij}(t+1) - x_{ij}(t)$. Then

$$\frac{1}{C}\sum_{\tau=1}^{C}\sum_{(i,j)\in\mathcal{A}^2} (x_{ij}(t+\tau+1))^2 - (x_{ij}(t+\tau))^2 = \frac{1}{C}\sum_{\tau=1}^{C}\sum_{(i,j)\in\mathcal{A}^2} (\delta_{ij}(t+\tau))^2 + \delta_{ij}(t+\tau)x_{ij}(t+\tau) \tag{53}$$

Because $\delta_{ij}(t) \le \sum_{(k,i)\in\mathcal{A}^2} Q_{ki}$ and Q_{ki} is bounded, $\frac{1}{C}\sum_{\tau=1}^{C}\sum_{(i,j)\in\mathcal{A}^2} \mathbb{E}\left[(\delta_{ij}(t+\tau))^2\right]$ is also bounded. Use the definition of $\delta_{ij}(t)$ to expand $\frac{1}{C}\sum_{\tau=1}^{C}\sum_{(i,j)\in\mathcal{A}^2} \delta_{ij}(t+\tau)x_{ij}(t+\tau)$:

$$\frac{1}{C}\sum_{\tau=1}^{C}\sum_{(i,j)\in\mathcal{A}^2} \delta_{ij}(t+\tau)x_{ij}(t+\tau) = \frac{1}{C}\sum_{\tau=1}^{C}\sum_{(i,j)\in\mathcal{A}^2} \left(\sum_{k\in\mathcal{A}} y_{ki}(t+\tau)p_{ij}(t+\tau) - y_{ij}(t+\tau)\right) x_{ij}(t+\tau) \tag{54}$$

$$= \frac{1}{C}\sum_{\tau=1}^{C}\sum_{(i,j)\in\mathcal{A}^2} y_{ij}(t+\tau)\left(\sum_{k\in\mathcal{A}} p_{jk}(t+\tau)x_{jk}(t+\tau) - x_{ij}(t+\tau)\right) \tag{55}$$

Taking the expected value,

$$\mathbb{E}\left[\frac{1}{C}\sum_{\tau=1}^{C}\sum_{(i,j)\in\mathcal{A}^2} y_{ij}(t+\tau)\left(\sum_{k\in\mathcal{A}} p_{jk}(t+\tau)x_{jk}(t+\tau)-x_{ij}(t+\tau)\right)\middle|\mathbf{x}(t)\right]$$
$$=\frac{1}{C}\sum_{\tau=1}^{C}\sum_{(i,j)\in\mathcal{A}^2} y_{ij}(t+\tau)\left(\sum_{k\in\mathcal{A}} \bar{p}_{jk}x_{jk}(t+\tau)-x_{ij}(t+\tau)\right)$$
$$=-\frac{1}{C}\sum_{\tau=1}^{C}\sum_{(i,j)\in\mathcal{A}^2} y_{ij}(t+\tau)w_{ij}(t+\tau) \tag{56}$$

Expand $y_{ij}(t+\tau)$:

$$-\frac{1}{C}\sum_{\tau=1}^{C}\sum_{(i,j)\in\mathcal{A}^2} y_{ij}(t+\tau)w_{ij}(t+\tau)=$$
$$-\frac{1}{C}\sum_{\tau=1}^{C}\sum_{(i,j)\in\mathcal{A}^2} s_{ij}(t+\tau)Q_{ij}(1-L_{ij}(t))w_{ij}(t+\tau)$$
$$+\frac{1}{C}\sum_{\tau=1}^{C}\sum_{(i,j)\in\mathcal{A}^2} (s_{ij}(t+\tau)Q_{ij}(1-L_{ij}(t))-y_{ij}(t+\tau))w_{ij}(t+\tau) \tag{57}$$

If $w_{ij}(t+\tau)\geq s_{ij}(t+\tau)Q_{ij}$ then $y_{ij}(t+\tau)=s_{ij}(t+\tau)Q_{ij}(1-L_{ij}(t))$, rendering that term equal to 0. Therefore,

$$\frac{1}{C}\sum_{\tau=1}^{C}\sum_{(i,j)\in\mathcal{A}^2} (s_{ij}(t+\tau)Q_{ij}(1-L_{ij}(t))-y_{ij}(t+\tau))w_{ij}(t+\tau)\leq\frac{1}{C}\sum_{\tau=1}^{C}(Q_{ij})^2=(Q_{ij})^2 \tag{58}$$

Continue working with $-\frac{1}{C}\sum_{\tau=1}^{C}\sum_{(i,j)\in\mathcal{A}^2} s_{ij}(t+\tau)Q_{ij}(1-L_{ij}(t))w_{ij}(t+\tau)$. Because $-Q_{ij}\leq x_{ij}(t+1)-x_{ij}(t)\leq-\sum_{k\in\mathcal{A}}Q_{ki}$, $w_{ij}(t+1)-w_{ij}(t)\leq-Q_{ij}-\sum_{k\in\mathcal{A}}Q_{kj}=\Delta_{ij}$.

$$-\frac{1}{C}\sum_{\tau=1}^{C}\sum_{(i,j)\in\mathcal{A}^2} s_{ij}(t+\tau)Q_{ij}(1-L_{ij}(t))w_{ij}(t+\tau)\leq-\frac{1}{C}\sum_{\tau=1}^{C}\sum_{(i,j)\in\mathcal{A}^2} s_{ij}(t+\tau)Q_{ij}(1-L_{ij}(t))(w_{ij}(t)+\Delta_{ij}) \tag{59}$$

Since $-\frac{1}{C}\sum_{\tau=1}^{C}\sum_{(i,j)\in\mathcal{A}^2} s_{ij}(t+\tau)Q_{ij}(1-L_{ij}(t))\Delta_{ij}$ is bounded, we are left with $-\frac{1}{C}\sum_{\tau=1}^{C}\sum_{(i,j)\in\mathcal{A}^2} s_{ij}(t+\tau)Q_{ij}(1-L_{ij}(t))w_{ij}(t)$. Since $\bar{\mathbf{d}}\in\mathcal{D}^0$, there exists some control $\bar{\mathbf{s}}\in\mathcal{S}$ such that Eq. (46) holds (Varaiya, 2013). By Lemma 2, Eq. (46) implies that

$$-\frac{1}{C}\sum_{\tau=1}^{C}\sum_{(i,j)\in\mathcal{A}^2}\bar{s}_{ij}Q_{ij}\left(1-\bar{L}_{ij}\right)w_{ij}(t)\leq\kappa-\epsilon|\mathbf{x}(t)| \tag{60}$$

$\bar{\mathbf{s}}$ may not correspond to a phase activation, but by Lemma 1,

$$-\frac{1}{C}\sum_{\tau=1}^{C}\sum_{(i,j)\in\mathcal{A}^2} s^{\star}_{ij}(t+\tau)Q_{ij}(1-L_{ij}(t))w_{ij}(t)\leq-\frac{1}{C}\sum_{\tau=1}^{C}\sum_{(i,j)\in\mathcal{A}^2}\bar{s}_{ij}Q_{ij}\left(1-\bar{L}_{ij}\right)w_{ij}(t) \tag{61}$$
$$\leq\kappa-\epsilon|\mathbf{x}(t)| \tag{62}$$

which achieves equation (52) for the max-pressure policy. □

Proposition 5. *If $\bar{\mathbf{d}}\in\mathcal{D}^0$, then the max-pressure policy is stabilizing.*

Proof. By Lemma 3,

$$\frac{1}{C}\sum_{\tau=1}^{C}\mathbb{E}\left[\sum_{(i,j)\in\mathcal{A}^2}(x_{ij}(t+\tau+1))^2-(x_{ij}(t+\tau))^2\middle|\mathbf{x}(t)\right]\leq\kappa-\epsilon|\mathbf{x}(t)| \tag{63}$$

Taking the sum over T on both sides,

$$\frac{1}{T}\sum_{t=1}^{T}\mathbb{E}\left[\frac{1}{C}\sum_{\tau=1}^{C}\sum_{(i,j)\in\mathcal{A}^2}(x_{ij}(t+\tau+1))^2-(x_{ij}(t+\tau))^2\right]\leq\frac{1}{T}\sum_{t=1}^{T}(\kappa-\epsilon|\mathbf{x}(t)|)$$

Simplifying,

$$\frac{1}{T}\mathbb{E}\left[\frac{1}{C}\sum_{\tau=1}^{C}\sum_{(i,j)\in\mathcal{A}^2}(x_{ij}(T+\tau+1))^2-(x_{ij}(\tau))^2\right]\leq\frac{1}{T}\sum_{t=1}^{T}(\kappa-\epsilon|\mathbf{x}(t)|) \tag{64}$$

$$\frac{\epsilon}{T}\sum_{t=1}^{T}|\mathbf{x}(t)| + \frac{1}{T}\mathbb{E}\left[\frac{1}{C}\sum_{\tau=1}^{C}\sum_{(i,j)\in\mathcal{A}^2}(x_{ij}(T+\tau+1))^2 - (x_{ij}(\tau))^2\right] \leq \kappa \tag{65}$$

Taking the limit as $T \to \infty$,

$$\lim_{T\to\infty}\left(\frac{\epsilon}{T}\sum_{t=1}^{T}|\mathbf{x}(t)| + \frac{1}{T}\mathbb{E}\left[\frac{1}{C}\sum_{\tau=1}^{C}\sum_{(i,j)\in\mathcal{A}^2}(x_{ij}(T+\tau+1))^2 - (x_{ij}(\tau))^2\right]\right) \leq \kappa \tag{66}$$

Simplifying,

$$\lim_{T\to\infty}\frac{\epsilon}{T}\sum_{t=1}^{T}|\mathbf{x}(t)| \leq \kappa \tag{67}$$

which results in $\lim_{T\to\infty}\frac{1}{T}\sum_{t=1}^{T}|\mathbf{x}(t)| \leq \frac{\kappa}{\epsilon}$. □

3.6. Discussion

It is important to qualify the context of the maximum stability result. The cyclical max-pressure policy has maximum stability among controls which follow the same constraints, namely that the signal phases are organized into a cycle of length C_n or less, each phase is actuated at least once per cycle, and the phases are actuated in a predefined order. These constraints reduce the size of the stability region, yet the cyclical max-pressure control achieves maximum stability within this reduced region. Nevertheless, the cyclical max-pressure control may not perform as well as previous controls (e.g. Varaiya, 2013). The purpose of defining this control is to satisfy practical considerations of city engineers and travelers, who may be unwilling to implement an unconstrained max-pressure control which can select phases in arbitrary order.

4. Numerical results

To test the effects of a cycle length on max-pressure intersection control, simulations on the downtown Austin city network (shown in Fig. 1) were conducted. The downtown Austin city network consists of 171 zones, 546 intersections, and 1247 links, and was calibrated to match observed morning peak characteristics in 2011 by the Network Modeling Center at The University of Texas at Austin. The network includes most of the central business district of Austin, Texas, as well as arterials north of the city and the two major north–south freeways. Simulations were performed with a time step of 15 s and a total duration of 3 h, with demand entering throughout the simulation. Demand followed the same origin–destination distribution pattern, but was uniformly scaled to explore stability. The original network includes signal phases for many intersections, and those same phases were used (with adjusted timings) in the cyclical max-pressure control. Lost times were 2 s per phase. The original demand is specified as 62,836 vehicles over 2 h. The network appears to be unstable at that demand, so scaled-down demands are used here. (Although the network is unstable at its original demand, the peak period has limited duration resulting in queue lengths dissipating as the peak period ends).

The numerical results presented here compare the cyclical max-pressure (hereafter referred to as CYCLE-MP) control to the non-cyclical max-pressure (referred to as MP) control of Varaiya (2013). We compare CYCLE-MP to MP on several metrics, including throughput and waiting times at intersections. It is important to note that we do not expect CYCLE-MP to perform better than MP in most metrics. The performance of CYCLE-MP is limited by the requirement to actuate each phase at least once per cycle and the exogenous phase selection. Actuating each phase at least once per cycle reduces the size of the stability region as per equation (7), and also creates delay between observing a queue and actuated a phase for it by constraint (28). Exogenous phase selection limits the set of phases that may be actuated to a predefined set of phases that are actuated in order, $\mathcal{P}_n$. $\mathcal{P}_n$ is a subset of all admissible phases for the cycle (as defined by the dual-ring controller). When $\mathcal{P}_n$ is a strict subset, some phases may be actuated by MP but not by CYCLE-MP. Obviously, these constraints will reduce performance. However, these constraints come with the significant practical benefit of cycle-based phases with max-pressure signal timing for maximum stability. Therefore, we interpret these numerical results as an evaluation of the performance costs of including a cyclical phase structure in the traffic signal.

4.1. Stability comparison

First, we compare the stability of the networks according to definition (8). Essentially, we evaluate whether the total number of vehicles in the network is increasing over time for different demand levels. Fig. 2 compares the network stability of MP and CYCLE-MP models with cycle lengths of 120 s and 450 s. Demand maintained the origin–destination proportions of the original calibrated network but was scaled up or down as necessary. At a demand rate of 18,000 vehicles per hour, all three policies appear to be stable with the number of vehicles in the network initially increasing then appearing to plateau at a constant. However, as the demand increases to up to 26,000 vehicles per hour, the traditional max-pressure control model remains stable but both of the cycle length models start becoming unstable. Unsurprisingly, MP has a larger stable region than CYCLE-MP and is therefore able to stabilize the network at higher demand levels. CYCLE-MP is limited both by actuating each phase at least once per cycle, and by the exogenously specified set of phases.

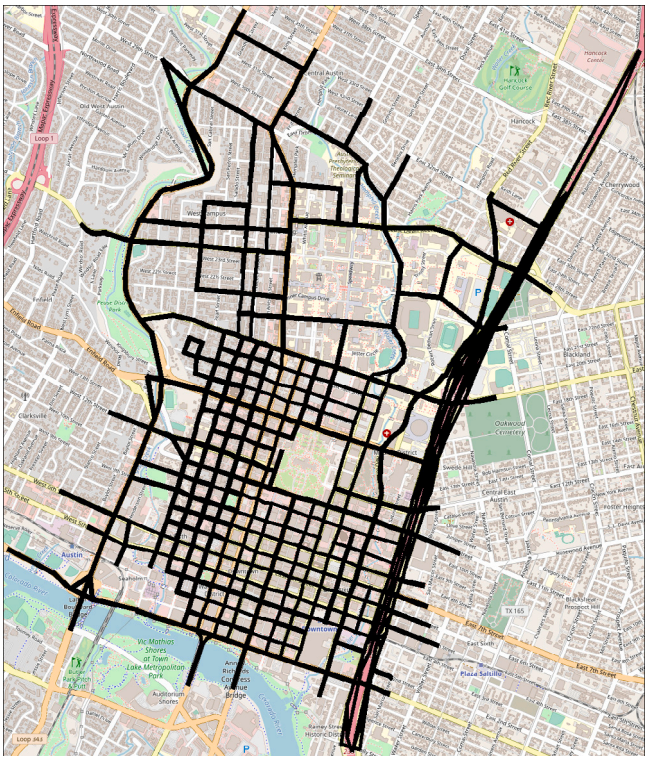

Fig. 1. Map of the downtown Austin city network.

Figs. 2(b) and 2(c) compare stability between CYCLE-MP with cycle length 120 s and 450 s. Recall that 120 s (respectively 450 s) is the maximum permissible cycle length, but smaller cycle lengths can be chosen in real-time by the CYCLE-MP controller. The results are very similar, with the cycle length of 120 s resulting in a slightly higher rate of increase. These minor differences are likely attributed to how actuating each phase at least once per cycle is not limiting in practical networks where demand arrives regularly from each approach. Fig. 2 suggests that the main limitation to the stable region occurs from the exogenous phase selection instead.

4.2. Travel times

Fig. 3 compares the average travel time of MP versus CYCLE-MP with cycle length of 225 s. Although vehicles in the modified max-pressure scenario have a higher average travel time, the difference is only around 3 min. Also, the difference in performance between the two models remains relatively constant as demand increases. The higher travel time is likely attributed to higher delays at intersections resulting from the requirement to actuate phases in order. This constraint can cause a delay of several time steps between observing a large queue and actuating the most appropriate phase for that queue.

Fig. 3 also compares the travel times of Le et al. (2015)'s method using the same cycle length of 225 s. Overall, Le et al. (2015)'s method was observed to be significantly worse than CYCLE-MP. We believe the differences are primarily due to CYCLE-MP shortening the cycle length adaptively in response to real-time demand. We can understand this behavior with the following example. Consider a 2-phase traffic signal with a cycle length of 120 s, and a 15 s time step, and for simplicity, assume no downstream queues. Suppose that demand is exactly 30veh/hr per phase, which is also 1veh per cycle per phase. If the pressure for each phase at time t was equal to 1, the proportional time controller of Le et al. (2015) would allocate 60 s to each phase. The vehicle queued for phase 1 receives 60 s green time, and the vehicle queued for phase 2 must wait 60 s. In contrast, CYCLE-MP would switch to phase 2 after the first time step, resulting in a waiting time of 15 s. The method of Le et al. (2015) would continue to allocate 60 s per phase, while CYCLE-MP would actuate the phase with the longer queue length every 15 s.

Fig. 4(a) shows the difference between the average travel time per link between MP and CYCLE-MP with cycle length of 225 s. The average travel time per link was computed and averaged across all links in the network, and the difference in that value between the two models is plotted. CYCLE-MP results in a higher travel time per link, however as demand increases the difference in average travel time is almost constant. The difference is also relatively small at around 1.5 s per link.

Fig. 4(b) shows the difference in link travel time between CYCLE-MP with cycle length of 225 s and MP, but with only the highest-delay link at every intersection. The highest-delay links were chosen using the MP scenario. Since CYCLE-MP actuates each phase at least once per cycle, the idea is to determine whether CYCLE-MP reduces delay for the highest-delay link at each intersection, which should be the link benefiting most from the cyclical phase structure. Surprisingly, CYCLE-MP has a higher delay than MP even on the

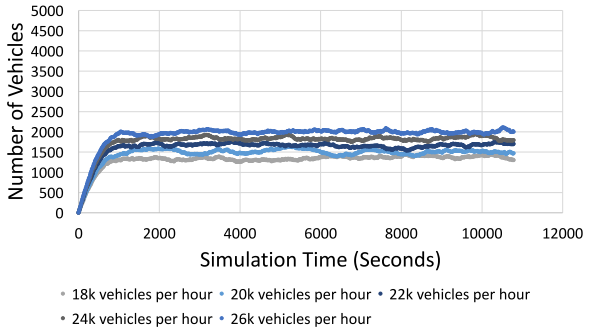

(a) No Cycle Length

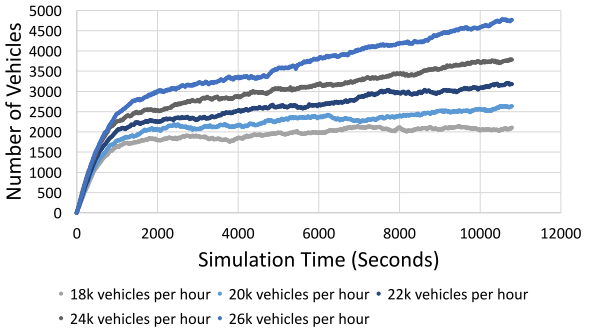

(b) Cycle Length of 120 seconds

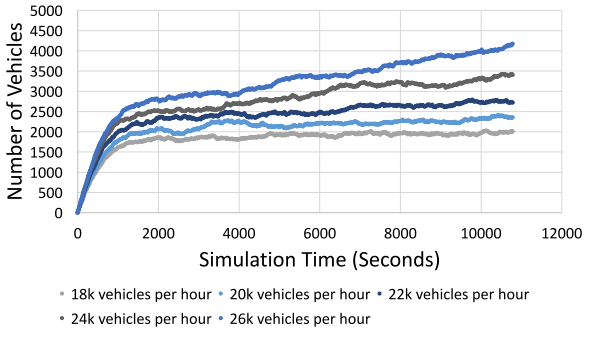

(c) Cycle Length of 450 seconds

Fig. 2. Network stability.

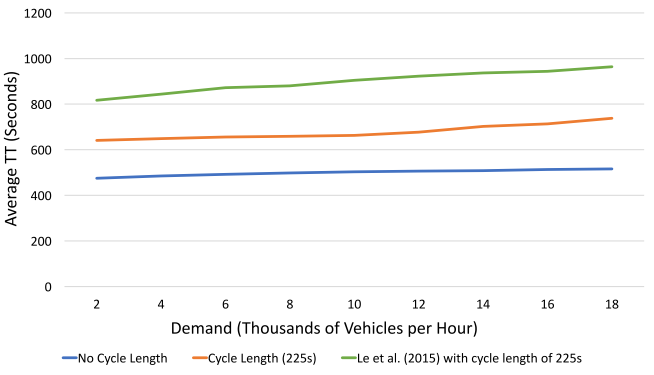

Fig. 3. Average travel time.

worst-performing links. However as demand increases the difference in performance appears to decrease. At lower demands, MP may naturally actuate each phase because demand is easily served. At higher demands, MP may be more likely to actuate phases for high-demand approaches, whereas CYCLE-MP ensures that low-demand approaches receive some green time each cycle.

4.3. Intersection waiting times

Fig. 5 shows the number of occurrences that a vehicle has to wait at an intersection for more than a certain amount of time between cycle max-pressure and regular max-pressure control. The graph is essentially a reverse cumulative distribution function. For every value of waiting time on the x axis, the corresponding count on the y axis is the total number of times vehicles have had to wait x or more seconds at an intersection throughout the duration of the simulation. Each vehicle is only counted once per intersection.

Fig. 5(a) shows the difference in intersection waiting times between CYCLE-MP with cycle length of 225 s and MP for a demand of 10,000 vehicles per hour. Although CYCLE-MP performs worse than MP for waiting times up to 180 s, the difference is not drastic and diminishes for waiting times more than 225 s. For waiting times greater than 180 s, almost no difference is observed. (Although

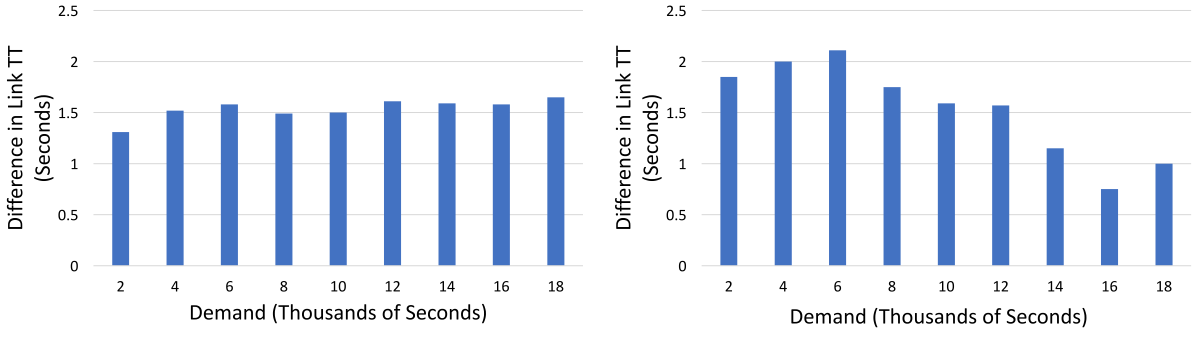

(a) All links (b) Worst performing link per intersection

Fig. 4. Link travel times.

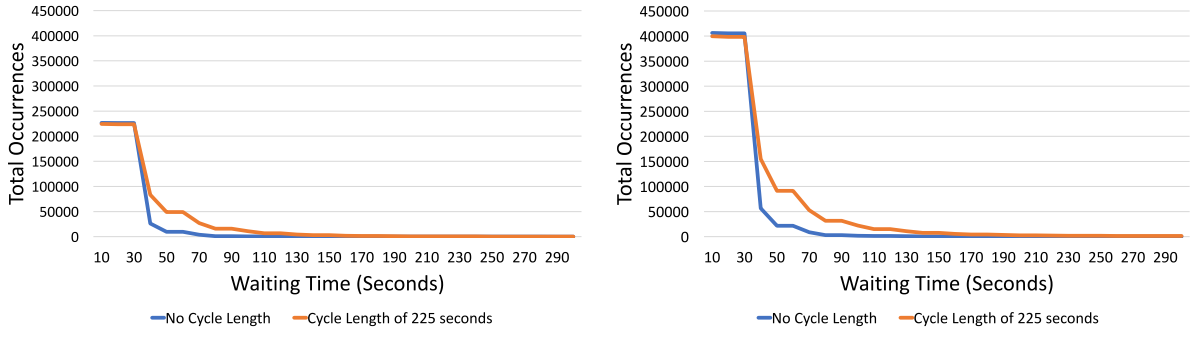

(a) Demand = 10k vehicles per hour (b) Demand = 18k vehicles per hour

Fig. 5. Intersection waiting times.

the cycle length is 225 s, greater delays are possible if capacity is insufficient for the queue.) Fig. 5(b) shows a similar trend for a demand of 18,000 vehicles per hour. These results suggest that higher waiting times for CYCLE-MP are mostly due to cycle-based delays in actuating the best phase, as expected for the cyclical phase structure.

Fig. 5 also includes results from the method of Le et al. (2015), and shows that the higher average travel times seen in Fig. 3 corresponds to higher intersection waiting times. This fits the explanation that the fixed cycle length results in higher vehicle delays when using Le et al. (2015)'s method. Higher intersection waiting times are observed for both 10,000 and 18,000 vehicles per hour. Even at higher demand levels, there are likely many intersections where the full 225 s cycle length is longer than needed to serve all demand, resulting in higher delays.

4.4. Comparing worst performing turns per intersection

Fig. 6 describes histograms of the average red light time for the turn at every intersection with the highest average red light time (determined from the MP scenario). The average red light time for every turn in the network was recorded, and the turns with the highest red light time for their respective intersections were added to the histograms. A maximum cycle length of 225 s was used for CYCLE-MP. These results are the most favorable for CYCLE-MP, as expected. Fig. 6(a) shows that with MP and a demand of 10,000 vehicles per hour, there are a significant amount of turns that have an average red light time of more than 400 s, while CYCLE-MP with a cycle length of 225 s there are no turns that have an average red light time of more than 225 s (as expected from the maximum cycle length). Fig. 6(b) shows that similar results are obtained with a demand of 18,000 vehicles per hour.

These results show the practical benefit achieved by CYCLE-MP: a reduction in the longest waiting time for any specific turning movement. As expected, in some scenarios MP will have a large waiting time because phase selection is arbitrary. Although MP is also more likely than CYCLE-MP to have a waiting time less than 50 s, it is also possible to have waiting times of greater than 400 s. Such waiting times could result in significant complaints by drivers and/or pedestrians waiting for a phase that actuates their crosswalk.

We further refine Fig. 6 by studying the waiting times of vehicles at the worst turn per intersection. Fig. 7(b) shows histograms of the average waiting time for the turn at every intersection with the highest average waiting time. The average waiting times for every turn in the network were recorded, and the turns with the highest average waiting time for their respective intersections (based on the MP scenario) were added to the histograms. Although Fig. 6 shows the longest red light (which could affect pedestrians),

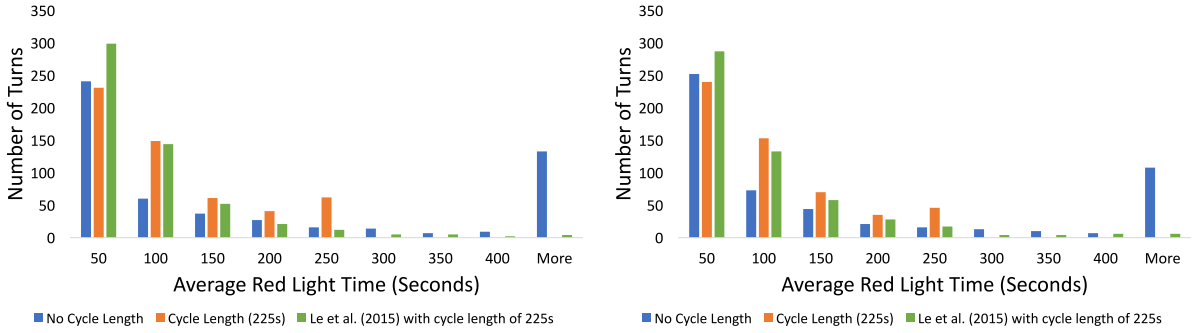

(a) Demand = 10k vehicles per hour (b) Demand = 18k vehicles per hour

Fig. 6. Red light times for worst performing turns.

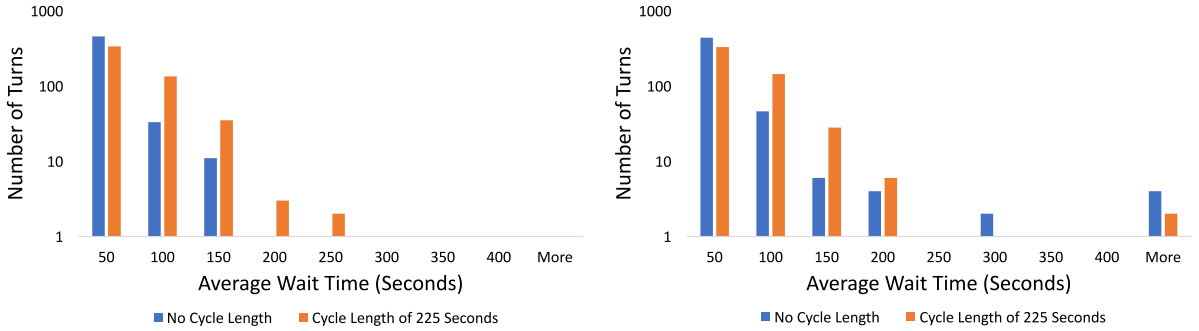

(a) Demand = 10k vehicles per hour (b) Demand = 18k vehicles per hour

Fig. 7. Waiting times for worst performing turns.

Fig. 7 shows the time that vehicles spend waiting. While a long red light time might be observed for one turning movement, if no vehicles are waiting for that turn it is less problematic (but could still affect pedestrians).

Fig. 7(a) shows that with a demand of 10,000 vehicles per hour, MP has better performance for the worst performing turns, with neither model having a single turn with more than 300 s of average waiting time. At low demand, the demand is much less than the capacity, which means that MP can often actuate phases soon after vehicles arrive. In some cases, CYCLE-MP must wait to actuate a phase due to the signal cycle. However, Fig. 7(b) shows that as we increase the demand to 18,000 vehicles per hour, both models have some turns that have a very high average waiting time, with MP having more turns with average waiting times of 300 s or more compared to CYCLE-MP with cycle length of 225 s. At high demand, MP prefers to actuate phases to serve long queues, whereas CYCLE-MP actuates each phase once per cycle. CYCLE-MP still has some high waiting times of greater than 400 s due to insufficient capacity for a long queue, but most waiting times are less than the cycle length.

5. Conclusions

Due to practical issues with implementing max-pressure control raised by city traffic engineers, this paper presents a revised max-pressure control in which phases are actuated in an exogenous ordering defining a signal cycle. The duration (number of time steps) that each phase is actuated is still decided by the max-pressure control, but a maximum cycle length constraint is imposed. Smaller cycle lengths can be chosen by the max-pressure control in response to real-time queues. Consequently, the stability region (set of demand rates that can be served) is reduced by both the constraint of a maximum cycle length and an exogenously-specified phase cycle. This stability region applies to any traffic signal timing that follows the maximum cycle length and exogenous phase cycle constraints. We define a modified max-pressure control and prove maximum stability under these constraints, meaning it can serve any demand in the stability region. The modified max-pressure control takes the form of a decentralized model predictive controller with a lookahead time of one cycle length. However, we prove that it can be solved by enumerating over phases, so it is no more computationally intensive than the max-pressure control of Varaiya (2013).

Numerical results on the downtown Austin city network suggest that in practical networks, the maximum cycle length constraint is not a major limitation on performance because demand arrives regularly from all approaches. The demand is therefore more balanced, and the extremes of the phase durations restricted by a maximum cycle length are not needed. However, the exogenously-specified phases seems to limit the stability region. Overall, performance is slightly worse with this cycle-based max-pressure control

than the original max-pressure control of Varaiya (2013), which is expected. The main benefits occur in how the constraints achieve a signal cycle that is acceptable to city engineers and travelers while retaining the analytical maximum stability result. Pedestrians waiting for crosswalk actuation should also benefit because a maximum cycle length results in a maximum waiting time for pedestrians, unlike the original max-pressure control (Varaiya, 2013). We hope that the analytical results will inspire rigorous methods for traffic engineers to implement max-pressure control while retaining practically-desirable behavior.

These results would benefit from additional numerical analyses on city networks in future work using microsimulation tools, like Sun and Yin (2018) did for standard max-pressure control. In addition, revising the flow model to use kinematic wave theory, like Li and Jabari (2019) would improve its applicability to traffic networks. Major advantages of using kinematic wave theory include links having finite queue buffers and travel speeds through links being affected by density Another possible extension is revising the cycle constraints so that each turning movement must be actuated at least once per cycle, but with potentially varying phases. Although the resulting traffic signal might not follow a recognizable cycle, it would still have the desirable characteristic of maximum waiting time for any turning movement.

CRediT authorship contribution statement

Michael W. Levin: Conceptualization, Methodology, Software, Validation, Writing. **Jeffrey Hu:** Software, Visualization, Writing. **Michael Odell:** Writing.

Acknowledgments

The authors gratefully acknowledge the support of the National Science Foundation, United States of America, Award No. 1935514 and the Minnesota Department of Transportation, United States of America.

References

Anderson, L., Pumir, T., Triantafyllos, D., Bayen, A.M., 2018. Stability and implementation of a cycle-based max pressure controller for signalized traffic networks. Netw. Heterog. Media 13 (2), 241.

Chen, R., Hu, J., Levin, M.W., Rey, D., 2020. Stability-based analysis of autonomous intersection management with pedestrians. Transp. Res. C 114, 463–483.

Dixit, V., Jayakumar, N., Chand, S., Levin, M.W., 2020. A simple crowdsourced delay-based traffic signal control. PLoS One.

Gregoire, J., Frazzoli, E., de La Fortelle, A., Wongpiromsarn, T., 2014a. Back-pressure traffic signal control with unknown routing rates. IFAC Proc. Vol. 47 (3), 11332–11337.

Gregoire, J., Qian, X., Frazzoli, E., De La Fortelle, A., Wongpiromsarn, T., 2014b. Capacity-aware backpressure traffic signal control. IEEE Trans. Control Netw. Syst. 2 (2), 164–173.

Le, T., Kovács, P., Walton, N., Vu, H.L., Andrew, L.L., Hoogendoorn, S.S., 2015. Decentralized signal control for urban road networks. Transp. Res. C 58, 431–450.

Le, T., Vu, H.L., Walton, N., Hoogendoorn, S.P., Kovács, P., Queija, R.N., 2017. Utility optimization framework for a distributed traffic control of urban road networks. Transp. Res. B 105, 539–558.

Levin, M.W., Rey, D., Schwartz, A., 2019. Max-pressure control of dynamic lane reversal and autonomous intersection management. Transportmetrica B: Transp. Dyn. 7 (1), 1693–1718.

Li, L., Jabari, S.E., 2019. Position weighted backpressure intersection control for urban networks. Transp. Res. B 128, 435–461.

Mercader, P., Uwayid, W., Haddad, J., 2020. Max-pressure traffic controller based on travel times: An experimental analysis. Transp. Res. C 110, 275–290.

Pumir, T., Anderson, L., Triantafyllos, D., Bayen, A.M., 2015. Stability of modified max pressure controller with application to signalized traffic networks. In: 2015 American Control Conference. ACC, IEEE, pp. 1879–1886.

Rey, D., Levin, M.W., 2019. Blue phase: Optimal network traffic control for legacy and autonomous vehicles. Transp. Res. B 130, 105–129.

Sun, X., Yin, Y., 2018. A simulation study on max pressure control of signalized intersections. Transp. Res. Rec. 2672 (18), 117–127.

Tassiulas, L., Ephremides, A., 1992. Stability properties of constrained queueing systems and scheduling policies for maximum throughput in multihop radio networks. IEEE Trans. Automat. Control 37 (12), 1936–1948.

Varaiya, P., 2013. Max pressure control of a network of signalized intersections. Transp. Res. C 36, 177–195.

Wongpiromsarn, T., Uthaicharoenpong, T., Wang, Y., Frazzoli, E., Wang, D., 2012. Distributed traffic signal control for maximum network throughput. In: 2012 15th International IEEE Conference on Intelligent Transportation Systems. IEEE, pp. 588–595.

Xiao, N., Frazzoli, E., Li, Y., Wang, Y., Wang, D., 2014. Pressure releasing policy in traffic signal control with finite queue capacities. In: Decision and Control (CDC), 2014 IEEE 53rd Annual Conference on. IEEE, pp. 6492–6497.